Fiber Laser Based Two-Photon FRET Measurement of Calmodulin and mCherry-E^{0}GFP Proteins

PETER ADANY,[1] CAREY K. JOHNSON,[2] AND RONGQING HUI[1]*
[1]*Department of Electrical Engineering and Computer Science, University of Kansas, Lawrence, Kansas 66045*
[2]*Department of Chemistry, University of Kansas, Lawrence, Kansas 66045*

KEY WORDS wavelength tuning; photonic crystal fiber; Alexa Fluor 488; Texas Red; green fluorescent protein

ABSTRACT The speed and accuracy of Förster resonance energy transfer (FRET) measurements can be improved by rapidly alternating excitation wavelengths between the donor and acceptor fluorophore. We demonstrate FRET efficiency measurements based on a fiber laser and photonic crystal fiber as the source for two-photon excitation (TPE). This system offers the potential for rapid wavelength switching with the benefits of axial optical sectioning and improved penetration depth provided by TPE. Correction of FRET signals for cross excitation and cross emission was achieved by switching the excitation wavelength with an electrically controlled modulator. Measurement speed was primarily limited by integration times required to measure fluorescence. Using this system, we measured the FRET efficiency of calmodulin labeled with Alexa Fluor 488 and Texas Red dyes. In addition, we measured two-photon induced FRET in an E^{0}GFP-mCherry protein construct. Results from one-photon and two-photon excitation are compared to validate the rapid wavelength switched two-photon measurements. *Microsc. Res. Tech. 00:000–000, 2011.*

INTRODUCTION

Förster resonance energy transfer (FRET) is a nonradiative energy transfer between two fluorophores (Förster, 1948; Stryer, 1978). In recent years, the development of novel dyes and fluorescent proteins that facilitate FRET has spurred the study of protein structure and interactions in fixed and live cells (Albertazzi et al., 2009; Clegg, 1992; Erickson et al., 2001; Hillesheim et al., 2006; Millington et al., 2007; Panchuk-Voloshina et al., 1999; Shaner et al., 2004). FRET efficiency between a donor and acceptor pair is defined as the ratio of the rate of energy transfer to the total decay rate of the donor. FRET efficiency provides a quantitative measure of fluorophore separation because it depends on the donor–acceptor distance as r^{-6}, r being in the range of 10–60 Å in common applications.

The FRET efficiency can be measured by (1) the change in lifetime of the donor in the presence of acceptor, (2) donor dequenching, i.e. the enhancement of donor emission when the acceptor is deactivated (e.g. by photobleaching), or (3) the relative emission yields of donor and acceptor (Clegg, 1992). The third method is the most common and generally the most straightforward, with much faster acquisition than lifetime correlation. Donor energy transfers via FRET to the acceptor, causing FRET-sensitized acceptor fluorescence. Quantifying the sensitized fluorescence requires tracking of donor and acceptor fluorescence under donor and acceptor excitation (Gordon et al., 1998; Youvan et al., 1997).

Care must be taken in particular to dissect spectrally overlapping contributions from donor and acceptor emission and to account for direct acceptor excitation (Chen et al., 2006; Dinant et al., 2008; Erickson et al., 2001; Periasamy and Diaspro, 2003). Corrections for spectral overlap are particularly important for two-photon excitation (TPE), where excitation spectra are often broader than their one-photon counterparts and therefore more likely to overlap.

Although one-photon FRET excitation is straightforward, two-photon excitation (TPE) is advantageous for imaging applications because of intrinsic optical sectioning (Denk et al., 1990). TPE has a number of additional advantages, such as the wide spectral separation of fluorescence from the excitation wavelength, reduced bulk photobleaching, and better penetration depth at longer wavelengths. In single-molecule or single-pair FRET measurements, alternating laser excitation of donor and acceptor (ALEX) (Kapanidis et al., 2004) (also termed pulsed interleaved excitation in applications with pulsed lasers (Müller et al., 2005)) has been implemented to control for the presence of an acceptor fluorophore. The issue of spectral overlap does not factor into fluorescence lifetime based techniques, e.g. FLIM-FRET (Millington et al., 2007).

High intensity pulses are required for two-photon excitation, and traditionally Ti:Sapphire lasers have been used for this purpose. The tuning speed of currently

*Correspondence to: Rongqing Hui, Department of Electrical Engineering and Computer Science, University of Kansas, 1520 West 15th Street, Lawrence, KS 66045, USA. E-mail: hui@eecs.ku.edu

Abbreviations used: ALEX, alternating laser excitation; BSA, bovine serum albumin; CaM, calmodulin; FRET, Förster resonance energy transfer; LC, liquid crystal; OPA, one-photon absorption; PBS, phosphate buffered saline; PCF, photonic crystal fiber; SSFS, soliton self frequency shift; TPE, two-photon excitation.

Received 12 July 2011; accepted in revised form 19 November 2011

Contract grant sponsor: National Institute of Health; Contract grant number: NIH-RR023142.

DOI 10.1002/jemt.22002

Published online in Wiley Online Library (wileyonlinelibrary.com).

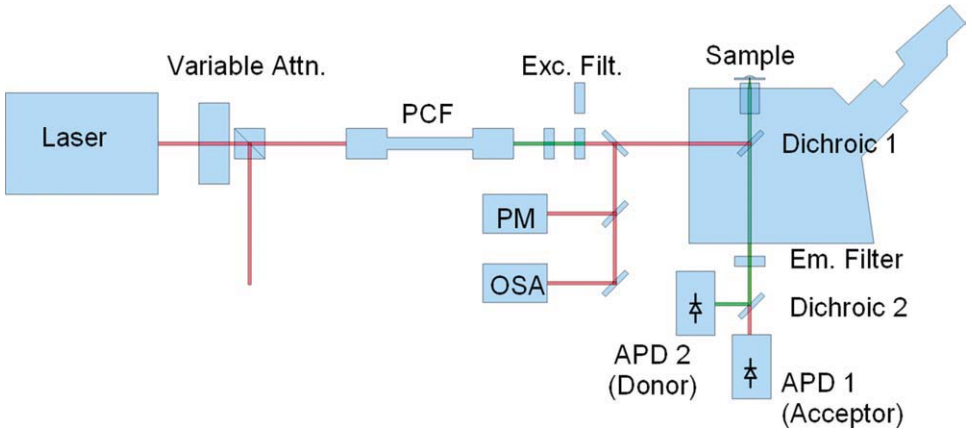

Fig. 1. FRET measurement components. Major components include a fiber laser, variable attenuator, a photonic crystal fiber (PCF), excitation filters, power meter (PM), optical spectrum analyzer (OSA), microscope dichroic (1), objective lens, emission filters, FRET dichroic (2), and avalanche photo diodes (APD 1, APD 2). Equipment and data collection were interfaced by a computer using Matlab. [Color figure can be viewed in the online issue, which is available at wileyonlinelibrary.com.]

available Ti:Sapphire systems is in the range of 40 nm/s. By contrast, tuning based on electro-optic modulation is nonmechanical and orders of magnitude faster. In order to increase speed and reduce the size and complexity of components in two- photon FRET measurements, we developed a two-photon excitation (TPE) based FRET system based on a turn-key femtosecond fiber laser and a photonic crystal fiber (PCF) that performs wavelength shifting of pulses through soliton self frequency shift (SSFS) (Adany et al., 2009; Unruh et al., 2006). This system provides electrically controlled wavelength tuning over a wide range, making it an ideal excitation source for two-photon FRET measurements and imaging. We performed wavelength switching with latencies of 10–20 ms using a liquid crystal modulator, although we previously demonstrated 5 μs switching times using a different electro-optic material (Adany et al., 2009).

Our goals are to demonstrate the feasibility of wavelength switching TPE for FRET using a PCF and to validate our techniques by recording FRET values for two model FRET constructs. To verify our techniques, we made FRET measurements of calmodulin labeled with fluorescent dyes Alexa Fluor 488 and Texas Red, as well as a mutant fluorescent protein with linked E^0GFP and mCherry (Albertazzi et al., 2009). Calmodulin is a valuable candidate for FRET study because it plays fundamental roles in all living cells and because it undergoes conformational changes on binding with calcium or specific target molecules (Allen et al., 2004). E^0GFP and mCherry are useful as they, along with the other families of fluorescent proteins, can be expressed and observed in living cells. To demonstrate the feasibility of our two-photon FRET measurement system, we measured proteins with rapidly alternating excitation over a wide range of excitation wavelengths. Our results include a comparison of FRET values obtained for calmodulin over the donor excitation wavelength range as well as time based observation of FRET of an E^0GFP-mCherry protein.

Thus, we present a practical FRET measurement system with the benefits of two-photon excitation, compact size and portability, and rapid wavelength switching for alternating excitation measurements leading to straightforward FRET analysis. Furthermore, using the continuous wavelength scanning capability of this system, we recorded two-photon excitation spectra of two sample FRET pairs.

MATERIALS AND METHODS

Two-Photon FRET Measurement With Fast Wavelength Tuning

The experimental setup is shown in Figure 1. The laser source (IMRA Femtolite-100) is a fiber-based femtosecond laser with a wavelength of 806 nm. The FWHM pulse width of the laser source is roughly 120 fs as measured using an autocorrelator (Femtochrome). The average output power is 100 mW and the pulse rate is 75 MHz, and therefore the pulse energy is 1.33 nJ with a peak power of ~11 kW. The transform-limited FWHM bandwidth, assuming sech^2 pulse shapes, is roughly 9 nm. The variable attenuator contains a voltage controlled liquid crystal (LC) birefringent cell (Meadowlark Optics) that rotates the polarization of the incoming vertically polarized light in reaction to a control voltage. The device is driven with a 2 kHz square voltage signal varied from 0 to 20 Vpp with zero DC offset. A polarization beam splitter transmits vertically polarized light toward the PCF while rejecting the horizontally polarized component. Pulses are then coupled into a Photonic Crystal Fiber (PCF) (Chroma NL-PM-750) to create wavelength shifted pulses through SSFS (Banaee and Young, 2006; Knight et al., 2000; Serebryannikov et al., 2005).

At the output of the PCF, a stable fundamental soliton is produced with a wavelength longer than the input pulse. The output wavelength depends on the length of the fiber (2 m) as well as the input power. Under higher input power, undesired higher order solitons are also created, and these components must be removed by excitation filters. Figure 2 is a waterfall plot that shows the measured soliton output spectrum over a range of soliton wavelengths. The fundamental

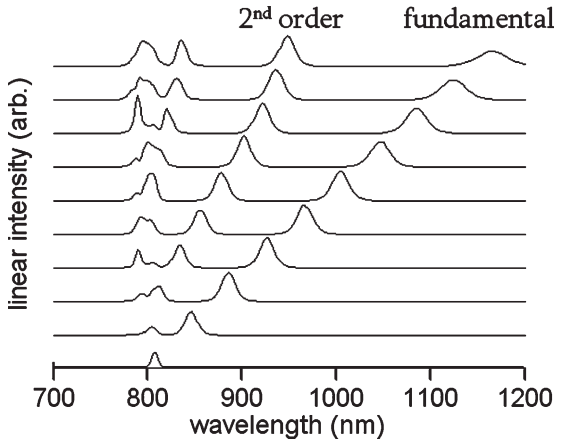

Fig. 2. Evolution of the soliton spectra when the input power is varied.

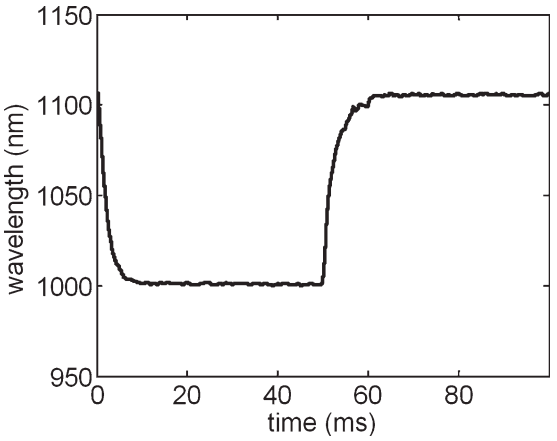

Fig. 3. Wavelength switching response as measured by a high speed photodiode. Values are interpolated from 100 measured values of soliton wavelength and photo current.

soliton can be tuned from ~850 nm to as far as 1,200 nm by varying the power of the input pulse at 806 nm. Below 850 nm, the coupled pulse power level drops steeply, whereas beyond 1,200 nm the output spectrum is significantly broadened and eventually develops into a supercontinuum. The parameters that contribute to the tunable range include the dispersion characteristic and length of the fiber as well as the width of the optical pulses. Hence, other wavelength ranges can be attained using different fiber types and input wavelengths. Note that as the wavelength of the fundamental soliton is tuned beyond 900 nm, a second order soliton starts to appear, which has to be filtered out by a long pass-filter in the experiment. In the measurements with wavelength scanning, we used a 950 nm long-pass filter when the soliton wavelength was between 975 nm and 1,050 nm, and we used a 1,000 nm long-pass filter for soliton wavelengths above 1,050 nm. The optimal filter cutoff wavelength for a given application can be determined from the spectral characteristic shown in Figure 2. For rapid wavelength switching, changing filters is not feasible and a single long-pass filter must accommodate the entire switched wavelength region as discussed later in this report.

Our system permits scanning a wide continuous wavelength range or rapid switching between two wavelengths. Targeting specific wavelengths involves calibrating the output pulse wavelength as a function of the input optical pulse power or control voltage. A demonstration of wavelength switching between ~1,000 and 1,100 nm is shown in Figure 3. The time response is limited by the response of the LC cell. The activation and relaxation times of the cell differ because of intrinsic material properties, the response time for activation (starting at time 0 ms in Fig. 3) is ~10 ms, and the relaxation time (starting at time 50 ms in Fig. 3) is ~20 ms. We have previously demonstrated faster switching times of roughly 5 μs with a PMT-PT modulator (Adany et al., 2009). While the PMT-PT material has much faster response, its electro-optic efficiency may vary over time at 800 nm, requiring more frequent calibration. The LC cell provided very good repeatability with standard deviation of 0.40 nm based on 50 trials. The pulse to pulse stability of the PCF soliton output can also be affected by intensity noise and power fluctuations of the pump laser. Based on the power-wavelength characteristic, a 0.1% RMS relative intensity noise would produce on the order of 0.2 nm RMS wavelength error. Therefore, this should not present a concern for this application.

The optical pulses at the PCF output pass through a bank of long-pass filters, which isolate the fundamental soliton and reject higher order solitons. A small fraction of the excitation light is sent to an optical power meter and optical spectrum analyzer for monitoring. The microscope (Olympus IX-71) houses a dichroic beam splitter (Chroma 800dcspxr) and objective lens (Olympus UPlanSApo 60x/1.20 Water Immersion). Because neither the dichroic beam splitter nor the lens is fully optimized for infrared wavelengths, their attenuation is stronger at 1,150 nm than at 850 nm by ~4 dB. Fluorescence emission passes back through the microscope dichroic splitter, a set of emission band-pass filters, and finally through a FRET dichroic splitter which discriminates donor and acceptor emission. Light is detected by avalanche photodiode photon counters (Micro Photon Devices PDM Series). We characterized crosstalk by measurements of reference dyes and by calculations based on profiles of the optical components.

Sample Preparation

The methods of preparation of calmodulin (CaM) labeled with Alexa Fluor 488 (AF-488) and Texas Red (TR) dyes were described in (Allen et al., 2004). A specimen was prepared by diluting 50 μL of CaM in 50 μL high calcium buffer. A 25 μL volume of this solution was placed on a 25 mm glass cover slip treated with bovine serum albumin (BSA). BSA was used to reduce adhesion of the protein to glass surfaces. The microscope focus was set 10 μm above the cover slip top surface. The concentration of CaM in the specimen was roughly

2.2 μM. Samples of the AF-488 and TR dye preparations were used for calibration.

The plasmid for E^0GFP-mCh was a kind gift from Dr. Lorenzo Albertazzi. Linked E^0GFP-mCherry (E^0GFP-mCh) FRET protein was developed by Albertazzi and coworkers (Albertazzi et al., 2009). The concentration of E^0GFP-mCh solution was ~2.0 μM. The fusion construct contains a thrombin enzyme cleavage site to allow separation of the two fluorophores. Cleaving eliminates FRET and thus provides calibration for the FRET efficiency measurement. The cleaving solution was prepared by combining 10 mL phosphate buffered saline (PBS) solution, 1,000 units of bovine thrombin and 1% *w/v* BSA. The E^0GFP-mCh sample was cleaved with one part by volume cleaving solution added to ten parts by volume protein solution. Roughly 86 units thrombin were used per milligram of protein, with a final thrombin concentration of about 9 units/mL. Alongside the thrombin sample, a FRET sample (no thrombin) was incubated in buffer solution of PBS with 1% *w/v* BSA added. Specimens were placed on glass cover slips under the same procedure as described for CaM.

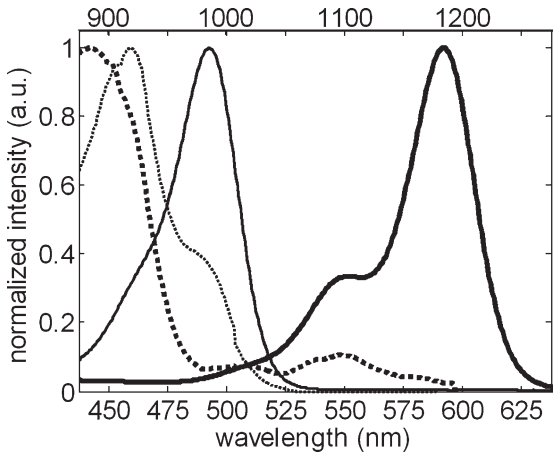

Fig. 4. Two-photon excitation (dashed) and one-photon absorption (solid) of Texas Red (in bold) and Alexa Fluor 488 (thin lines). Horizontal axis: OPA wavelength (bottom), TPE wavelength (top). TPE spectra were measured using the FRET measurement system. Traces are normalized.

Calculation of Experimental FRET Efficiency From Fluorescence Intensities

FRET efficiency can be expressed as

$$E = \frac{F_A}{F_A + G \cdot F_D} \tag{1}$$

where F_A is the sensitized acceptor fluorescence, F_D is the donor fluorescence and the factor G accounts for donor versus acceptor detector efficiency and quantum yields (Clegg, 1992).

Overlapping Emission. The fluorescence F_A is measured primarily as counts in one photo detector, C_1, while F_D is measured primarily in C_2. We use a simple matrix notation to describe the relationship between detector counts and fluorescence. Using this notation we incorporate cross talk terms in a matrix S and background counts Bg_1 and Bg_2 as

$$\begin{bmatrix} C_1 \\ C_2 \end{bmatrix} = \begin{bmatrix} S_{1A} & S_{1D} \\ S_{2A} & S_{2D} \end{bmatrix} \cdot \begin{bmatrix} F_A \\ F_D \end{bmatrix} + \begin{bmatrix} Bg_1 \\ Bg_2 \end{bmatrix} \tag{2}$$

Elements of S are products of the various filter transmission curves, fluorophore emission spectra and detector responsivity, with one of four possible combinations, e.g.

$$S_{1D}(\lambda) = C_{\text{norm}} \cdot \ \Re_1(\lambda)\, H_1(\lambda)\, H_O(\lambda) I_D(\lambda) \tag{3}$$

where $\Re_1$ is the responsivity of the first (acceptor) photo detector, H_1 is the FRET dichroic filter transmission to the first photo detector, H_O is the transmission of the objective optics (common to all), $I_D(\lambda)$ is the donor emission spectrum normalized to unity area, and C_{norm} is a normalizing constant. Transmission curves were generally held in data format, so S_{1D}, etc., were found by numeric integration over the relevant wavelength range. Inverting S leads to the following equation to determine fluorescence values:

$$\begin{bmatrix} F_A \\ F_D \end{bmatrix} = K \cdot \begin{bmatrix} S_{2D} & -S_{1D} \\ -S_{2A} & S_{1A} \end{bmatrix} \cdot \begin{bmatrix} C_1 - Bg_1 \\ C_2 - Bg_2 \end{bmatrix} \tag{4}$$

The value of the constant K can be disregarded since it can be factored out in the efficiency equation. Since S is normalized, quantum yield differences and system bias between acceptor and donor responses can be lumped into the factor G, which can be measured experimentally. We evaluated G according to the approach of (Chen et al., 2006), using measurements from a pair of samples, one with FRET and the other with no FRET, but otherwise identical in excitation and emission spectra and relative concentrations. From these samples we recorded ΔF_A and ΔF_D, the changes in fluorescence between the two samples taken under donor excitation, taking $G = \Delta F_A / \Delta F_D$.

Comparing crosstalk values calculated from emission spectra and filter transmission curves to those measured for the individual dyes, we found agreement within 3.0%. The measured crosstalk from AF-488 emission to the acceptor channel was 9.1%, and crosstalk from Texas Red emission to the donor channel was 2.9%. Since we could not measure separate E^0GFP and mCherry proteins, the calculated values (5.2% donor emission to acceptor channel and 4.8% acceptor emission to donor channel) were used.

Overlapping Excitation. In determining F_A and F_D, Eq. (4) corrects for crossemission but does not account for crossexcitation. In particular, the Texas Red two-photon excitation band overlaps the TPE peak of Alexa Fluor 488 as shown in Figure 4. The fraction of acceptor fluorescence caused by this direct excitation could not be measured directly, but it could be extrapolated by taking acceptor fluorescence under acceptor excitation and scaling it by γ, the ratio between the TPE cross section of Texas Red at the donor and

acceptor excitation wavelength. The FRET sensitized acceptor fluorescence was calculated as

$$F_A = F_{Ad} - \gamma F_{Aa} \quad (5)$$

where F_{Ad} and F_{Aa} are the measured acceptor fluorescence during excitation at donor and acceptor wavelengths, respectively.

It is useful to compare our methods with the three-cube method (Chen et al., 2006; Erickson et al., 2001), in which measurements of F_{Dd}, F_{Ad}, and F_{Aa} are made with alternating filter sets and a single photo detector. As discussed in (Erickson et al., 2001), in three-cube FRET correction for donor emission in the acceptor channel is made by calculations analogous to Eq. (4), while signal from acceptor emission in the donor channel is mitigated with narrow band emission filters. Note that we did not use individual narrow band emission filters, relying only on the dichroic beam splitter as a wavelength discriminator. Using two detectors, we measured donor and acceptor emission simultaneously, and the excitation wavelength was switched electronically so as to obtain all four signals, F_{Dd}, F_{Ad}, F_{Aa}, and F_{Da}. We thus corrected all emission cross talk by the matrix calculation of Eq. (4). This approach can compensate a great degree of emission overlap in the detectors, allowing wider bandwidth emission windows and hence somewhat higher signal levels. Most importantly, it eliminates the need to alternate filter sets during measurement.

The peak two-photon excitation (TPE) wavelengths of the FRET fluorophores were found by scanning the excitation wavelength over a wide continuous range. To calculate TPE spectra, average dark counts were subtracted and intensities were normalized by the square of the measured excitation power. Excitation power and wavelength were monitored as described above.

RESULTS

Two-Photon Excitation Spectra of Texas Red and Alexa Fluor 488

Two-photon excitation spectra are shown in Figure 4 for Texas Red and Alexa Fluor 488 dyes used in labeling calmodulin. For the purpose of comparison, the one-photon absorption (OPA) spectra measured with a UV-Visible Spectrophotometer (Agilent Cary-100) are also shown in the same figure. In agreement with general TPE characteristics, prominent spectral components of the OPA align with components of the TPE spectra on a double wavelength scale. The relative intensity of bands are generally different in two-photon and one-photon excitation, specifically with spectral intensity in two-photon excitation shifted to vibronic bands, leading to a blue shift in the peak of the two-photon excitation spectrum compared with the one-photon absorption spectrum, as noted previously (Albota et al., 1998a,b; Xu and Webb, 1996). While few examples of AF-488 or Texas Red TPE spectra are available in the literature, we note that the TPE excitation spectrum of Alexa Fluor 488 presented here differs from that given in (Bestvater et al., 2002).

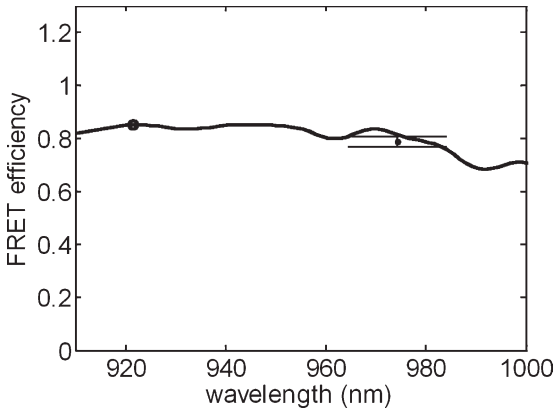

Fig. 5. CaM FRET efficiency versus donor excitation wavelength. The circle marks the optimal wavelength choice of 922 nm, corresponding to the peak two-photon excitation of AF-488. The point marker with error bars shows the results of switched wavelength measurement, which was made at 974 nm to avoid producing higher order solitons within the pass band of a single excitation filter set in place.

FRET Efficiency of Calmodulin With Alexa Fluor 488 and Texas Red

In order to resolve any uncertainty in accounting for the strongly overlapped TPE of Texas Red and AF-488 near 900 nm, we varied the donor excitation wavelength over a broad range. The dependence of calculated FRET efficiency on the choice of donor excitation wavelengths is shown in Figure 5.

The continuous line in Figure 5 was obtained by slowly scanning the wavelength of donor excitation; it provided the baseline to validate the results of wavelength switched FRET. As expected, the measured FRET efficiency shows little variation over the region of strong two-photon excitation of AF-488 and only shows a marked deviation in the region of weak two-photon cross section at wavelengths greater than 980 nm.

Our value of 0.85 for CaM two-photon FRET efficiency measured at 920 nm excitation wavelength is in close agreement with the previously reported value of 0.87 based on single photon excitation (Slaughter et al., 2005). Moreover, the broad wavelength scan validated the reliability of FRET measurement away from the peak donor TPE, at longer wavelengths. This verified that we could perform fast wavelength switched FRET in a longer-wavelength region and thus avoid the need to change the long-pass filter during the measurement.

FRET Efficiency of Linked E^0GFP & mCherry

The FRET efficiency of E^0GFP-mCh measured using two-photon excitation was 0.27, in good agreement with our one-photon result (0.29) for the same sample. For calibration purposes, a sample of E^0GFP-mCh was cleaved with thrombin enzyme. The emission spectra of E^0GFP-mCh before and after thrombin cleavage are shown in Figure 6, showing the effect of FRET on the emission spectrum.

It appears that cleavage was complete because no observable acceptor emission remained, as shown by

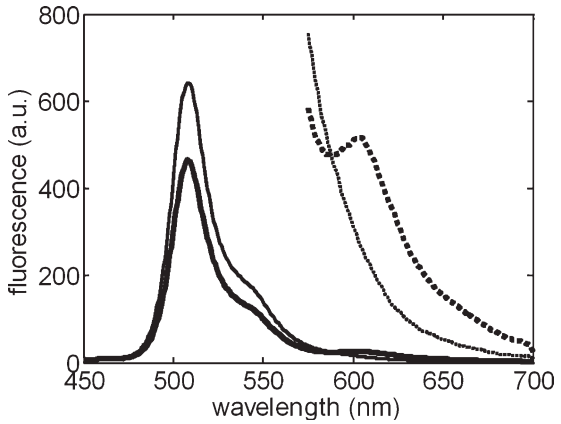

Fig. 6. Fluorescence spectra of E^0GFP-mCh with and without cleaving. The bold line shows E^0GFP-mCh fluorescence with FRET. Narrow line shows fluorescence of the cleaved sample (no FRET). Dashed lines are the same respective traces but magnified 20×.

TABLE 1. Summary of CaM FRET

Calmodulin	FRET efficiency	Separation, r (Å)	Excitation wavelengths (don./acc.)
Two-photon, λ-scanned	0.85	39	922 nm/1103 nm
Two-photon, λ-switched	0.78 ± 0.02	41	974 nm/1097 nm

TABLE 2. Summary of E^0GFP-mCh FRET

E^0GFP-mCherry	FRET efficiency	Separation, r (Å)	Excitation wavelengths (don./acc.)
One-photon	0.29	59	400 nm/586 nm
Two-photon, λ-scanned	0.27%	60	963 nm/1077 nm
Two-photon, λ-switched	0.28 ± 0.022	61	964 nm/1102 nm

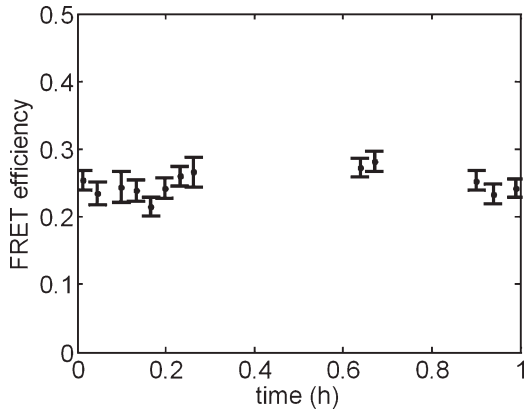

Fig. 7. FRET efficiency of E^0GFP-mCh with 13 data sets (each point represents 50 measurements) gathered over the course of 1 hr.

the 20× magnified traces in Figure 6. The difference between our result and the FRET efficiency of 0.35 previously reported in Albertazzi et al. (2009) could be explained by the presence of unlinked E^0GFP in the sample; however, any presence of unlinked acceptor (mCherry) should not affect the results.

The results of various FRET efficiency measurements of CaM and E^0GFP-mCh are summarized in Tables 1 and 2. Values of the Förster radius were 52 Å for CaM and 51 Å for E^0GFP-mCh (Albertazzi et al., 2009).

Wavelength Switching Two-Photon FRET Measurement of CaM and E^0GFP-mCh

To investigate the capability of fast wavelength switching in this system, we made wavelength-switched FRET measurements of both CaM and E^0GFP-mCh. Control voltages were calibrated to obtain the desired donor and acceptor wavelengths. Repeated tests of the voltage–wavelength characteristic confirmed that the calibration remained stable for at least 1 hr. Tracking the power levels confirmed that excitation wavelengths stayed entirely within ± 3 nm with respect to the targeted values over the course of each experiment. Photon counts were taken with 0.1 s integration. In Figure 5, the point marked with error bars shows the FRET measured with switched excitation between 974 and 1,097 nm. These wavelengths were chosen to accommodate a fixed 950 nm long-pass optical filter in the system to reject the high order solitons.

The limitation of donor excitation range was not a concern for E^0GFP-mCh, because its donor excitation peak is at a longer wavelength than that of CaM, and therefore we switched the excitation wavelength between 964 and 1,102 nm in the measurement. The resulting wavelength-switched two-photon FRET efficiencies of 0.78 ± 0.02 for CaM and 0.28 ± 0.022 for E^0GFP-mCh are consistent with the results of wavelength scanned measurements, as shown in Tables 1 and 2.

Figure 7 shows the FRET efficiency of E^0GFP-mCh measured over the course of an hour. The average FRET efficiency of E^0GFP-mCh did not vary significantly. Since donor fluorescence can change because of varying concentration, pH or other factors, the value of F_D in Eq. (1) was tracked throughout measurements by gauging changes in the acceptor fluorescence compared with the reference acceptor fluorescence from the cleaved sample. The remaining fluctuations shown in Figure 7 are primarily because of noise in the collected fluorescence signals.

DISCUSSION

We can conclude that the system measures FRET consistently and with a degree of accuracy comparable with other methods. The maximum measurement speed was primarily limited by low fluorescence levels, a factor tied to the relatively low excitation power. With 0.1 s integration time per excitation wavelength, along with the added latencies of wavelength switching and the computer acquisition procedure, the overall measurement rate was roughly 1 Hz. The wavelength was switched within 10–20 ms as shown in Figure 3, and as previously discussed the technique allows much faster modulation depending on the choice of electro-optic modulator. The remaining latency of about 0.4 s, attributed to the computer acquisition procedure, could be greatly reduced by

streamlining the hardware control, as the amount of data transferred is very small. Therefore, in principle the system has a capacity to reach 5 Hz as limited by 100 ms signal integration times. This system could be used for imaging by raster scanning of the sample, with point by point FRET analysis. The imaging time, proportional to the measurement rate, would be generally acceptable for stable samples. The advantages of using this class of laser still outweigh the practical obstacles of higher power lasers for many uses, and in the future the TPE rates could be increased thanks to recent improvements in fiber SSFS efficiency (van Howe et al., 2007).

We have demonstrated a FRET measurement technique using two-photon excitation with rapid wavelength switching. We measured two-photon excitation spectra of Alexa Fluor 488 and Texas Red dyes using continuous wavelength scanning between 850 and 1,175 nm along with their one-photon absorbances. We compared FRET efficiency values of two proteins (calmodulin and an E^0GFP-mCh construct) under different excitation wavelengths, with wavelength switching as well as broad donor wavelength scanning in the same system. Electronic wavelength switching simplifies the two-photon FRET measurement process and eliminates the need to alternate filters for calibration. The advantages of the system described here are the lower cost, greater portability, and more rapid tunability of the excitation source compared with conventional TPE excitation sources. Our results demonstrate the potential of practical two-photon FRET measurement based on rapid wavelength switching.

ACKNOWLEDGMENTS

The authors thank Dr. Lorenzo Albertazzi for providing the E^0GFP-mCherry plasmid.

REFERENCES

Adany P, Price ES, Johnson CK, Zhang R, Hui R. 2009. Switching of 800 nm femtosecond laser pulses using a compact PMN-PT modulator. Rev Sci Instrum 80:033107.

Albertazzi L, Arosio D, Marchetti L, Ricci F, Beltram F. 2009. Quantitative FRET analysis with the EGFP-mCherry fluorescent protein pair. Photochem Photobiol 85:287–97.

Albota M, Beljonne D, Bredas JL, Ehrlich JE, Fu JY, Heikal AA, Hess SE, Kogej T, Levin MD, Marder SR, McCord-Maughon D, Perry JW, Rockel H, Rumi M, Subramaniam G, Webb WW, Wu XL, Xu C. 1998a. Design of organic molecules with large two-photon absorption cross sections. Science 281:1653–1656.

Albota MA, Xu C, Webb WW. 1998b. Two-photon fluorescence excitation cross sections of biomolecular probes from 690 to 960 nm. Appl Opt 37:7352–7356.

Allen MW, Urbauer RJ, Johnson CK. 2004. Single-molecule assays of calmodulin target binding detected with a calmodulin energy-transfer construct. Anal Chem 76:3630–3637.

Banaee MG, Young JF. 2006. High-order soliton breakup and soliton self-frequency shifts in a microstructured optical fiber. J Opt Soc Am B 23:1484–1489.

Bestvater F, Spiess E, Stobrawa G, Hacker M, Feurer T, Porwol T, Berchner-Pfannschmidt U, Wotzlaw C, Acker H. 2002. Two-photon fluorescence absorption and emission spectra of dyes relevant for cell imaging. J Microsc 208(Pt 2):108–115.

Chen H, Puhl HL, III, Koushik SV, Vogel SS, Ikeda SR. 2006. Measurement of FRET efficiency and ratio of donor to acceptor concentration in living cells. Biophys J 91:L39–L41.

Clegg RM. 1992. Fluorescence resonance energy transfer and nucleic acids. Methods Enzymol 211:353–388.

Denk W, Strickler JH, Webb WW. 1990. Two-photon laser scanning fluorescence microscopy. Science 248:73–76.

Dinant C, van Royen ME, Vermeulen W, Houtsmuller AB. 2008. Fluorescence resonance energy transfer of GFP and YFP by spectral imaging and quantitative acceptor photobleaching. J Microsc 231(Pt 1):97–104.

Erickson MG, Alseikhan BA, Peterson BZ, Yue DT. 2001. Preassociation of calmodulin with voltage-gated Ca(2+) channels revealed by FRET in single living cells. Neuron 31:973–985.

Förster T. 1948. Zwischenmolekulare Energiewanderung und Fluoreszenz. Annalen der Physik 437:55–75.

Gordon GW, Berry G, Liang XH, Levine B, Herman B. 1998. Quantitative fluorescence resonance energy transfer measurements using fluorescence microscopy. Biophys J 74:2702–2713.

Hillesheim LN, Chen Y, Muller JD. 2006. Dual-color photon counting histogram analysis of mRFP1 and EGFP in living cells. Biophys J 91:4273–4284.

Kapanidis AN, Lee NK, Laurence TA, Doose S, Margeat E, Weiss S. 2004. Fluorescence-aided molecule sorting: Analysis of structure and interactions by alternating-laser excitation of single molecules. Proc Natl Acad Sci U S A 101:8936–8941.

Knight JC, Arriaga J, Birks TA, Ortigosa-Blanch A, Wadsworth WJ, Russell PSJ. 2000. Anomalous dispersion in photonic crystal fiber. IEEE Photonics Technol Lett 12:807–809.

Millington M, Grindlay GJ, Altenbach K, Neely RK, Kolch W, Bencina M, Read ND, Jones AC, Dryden DT, Magennis SW. 2007. High-precision FLIM-FRET in fixed and living cells reveals heterogeneity in a simple CFP-YFP fusion protein. Biophys Chem 127:155–164.

Müller BK, Zaychikov E, Brauchle C, Lamb DC. 2005. Pulsed interleaved excitation. Biophys J 89:3508–3522.

Panchuk-Voloshina N, Haugland RP, Bishop-Stewart J, Bhalgat MK, Millard PJ, Mao F, Leung WY. 1999. Alexa dyes, a series of new fluorescent dyes that yield exceptionally bright, photostable conjugates. J Histochem Cytochem 47:1179–1188.

Periasamy A, Diaspro A. 2003. Multiphoton microscopy. J Biomed Opt 8:327–328.

Serebryannikov EE, Hu ML, Li YF, Wang CY, Wang Z, Chai L, Zheltikov AM. 2005. Enhanced soliton self-frequency shift of ultrashort light pulses. J Exp Theor Phys Lett 81:487–490.

Shaner NC, Campbell RE, Steinbach PA, Giepmans BN, Palmer AE, Tsien RY. 2004. Improved monomeric red, orange and yellow fluorescent proteins derived from Discosoma sp. red fluorescent protein. Nat Biotechnol 22:1567–1572.

Slaughter BD, Unruh JR, Price ES, Huynh JL, Bieber Urbauer RJ, Johnson CK. 2005. Sampling unfolding intermediates in calmodulin by single-molecule spectroscopy. J Am Chem Soc 127:12107–12114.

Stryer L. 1978. Fluorescence energy transfer as a spectroscopic ruler. Annu Rev Biochem 47:819–846.

Unruh JR, Price ES, Molla RG, Stehno-Bittel L, Johnson CK, Hui R. 2006. Two-photon microscopy with wavelength switchable fiber laser excitation. Opt Express 14:9825–9831.

van Howe J, Lee JH, Zhou S, Wise F, Xu C, Ramachandran S, Ghalmi S, Yan MF. 2007. Demonstration of soliton self-frequency shift below 1300 nm in higher-order mode, solid silica-based fiber. Opt Lett 32:340–342.

Xu C, Webb WW. 1996. Measurement of two-photon excitation cross sections of molecular fluorophores with data from 690 to 1050 nm. J Opt Soc Am B 13:481–491.

Youvan DC, Silva CM, Bylina EJ, Coleman WJ, Dilworth MR, Yang MM. 1997. Calibration of fluorescence resonance energy transfer in microscopy using genetically engineered GFP derivatives on nickel chelating beads. Biotechnology et alia 3:1–18.